Proceedings of the
47th IEEE Conference on Decision and Control
Cancun, Mexico, Dec. 9-11, 2008

Instability Mechanisms in Cooperative Control

He Bai and Murat Arcak

Abstract— **We consider a motion coordination problem with second order agent dynamics and examine the closed-loop robustness with respect to switching topology, variation of link gain, and unmodeled dynamics. In each case, we illustrate with examples possible instability mechanisms and discuss under what conditions stability is maintained.**

I. Introduction

Motion coordination problems have been intensively studied during the past years, leading to significant results in formation control, flocking, and consensus [1], [2], [3], [4], [5], [6], [7], [8]. One of the challenges in the coordination problem is the design of local rules that guarantee the desired group behavior. The design and analysis of such rules make use of graph theory and potential function methods. The communication topology between agents is represented by a graph while the interactions between agents are modeled as artificial attraction/repulsion forces. The stability results follow from a Lyapunov function constructed from potential functions with the help of spectral properties of the graph Laplacian.

When the velocities of the agents are directly manipulatable, first-order kinematic models [1], [3] are appropriate. However, in many applications, only the acceleration of the agents can be controlled by input forces and torques, thereby leading to second or higher order dynamics [2], [5], [7], [8] with mass inertia incorporated.

In this paper, we consider double integrator agent dynamics with an undirected communication topology. We first analyze a cooperative system with a switching communication topology. Such switching may occur due to the vehicles joining or leaving a formation, transmitter/receiver failures, limited communication/sensor range, or physical obstacles temporarily blocking sensing between vehicles. For single integrator dynamics, switching topology has been studied in [1], [3] and stability under arbitrary switching has been ascertained for classes of coordination algorithms. In contrast, for second order dynamics, we illustrate with an example that a switching sequence that triggers instability exists. We then show that stability is maintained when switching is sufficiently fast or slow so that is does not interfere with the natural frequencies of the group dynamics.

This work is supported in part by by the Air Force Office of Scientific Research under award No. FA9550-07-1-0308.

He Bai is with the Department of Electrical, Computer and Systems Engineering, Rensselaer Polytechnic Institute, Troy, NY, USA. baih@rpi.edu

Murat Arcak is with Faculty of Electrical, Computer and Systems Engineering, Rensselaer Polytechnic Institute, Troy, NY, USA. He is also with Faculty of Electrical Engineering and Computer Sciences, University of California, Berkeley. arcakm@rpi.edu.

We next investigate stability properties when the link weights are perturbed by small sinusoidal oscillations. Perturbations of link weights may result from quantization and noise in the communication channels. In this paper we make a simplifying assumption that the perturbation is sinusoidal and transform the group dynamics into a form that reveals a parametric resonance mechanism [9], [10], [11]. This transformation employs the spectral properties of the graph Laplacian and decouples the relative motion from the motion of the center of the agents. When mass inertia and damping terms are identical for all agents, we obtain decoupled *Mathieu equations* [10], which make parametric resonance explicit. For broader classes of mass and damping matrices, we obtain coupled Mathieu equations and discuss which frequencies lead to parametric resonance. Next, we show that sinusoidal perturbations do not destabilize the system if they are slow or fast enough.

We finally study the effect of input unmodeled dynamics, such as fast actuator dynamics. Following standard singular perturbation arguments [12], we prove that the stability of the nominal design that ignores the effects of unmodeled dynamics is preserved when the stable unmodeled dynamics are sufficiently fast. As we illustrate with an example, how fast the unmodeled dynamics must be is dictated by the graph structure and the mass inertia matrix.

The subsequent sections are organized as follows: Section II introduces the nominal system and discusses its stability properties. We illustrate our instability example due to switching in Section III-A, followed by a discussion on when stability is maintained in Section III-B. We present a parametric resonance example in Section IV-A, which exhibits decoupled Mathieu equations, and generalize it to coupled Mathieu equations in Section IV-B. We then investigate the effects of fast and slow sinusoidal perturbations in Sections IV-C and IV-D. One of the contributions of Section IV is to introduce parametric resonance, which is a well-studied topic in structural mechanics, to cooperative control. Section V studies unmodeled dynamics.

II. Nominal Cooperative System and its Stability

We consider a group of agents which are represented by the vectors $x_i \in \mathbb{R}^p$, $i = 1, \cdots, n$ and their communication structure is represented with a graph. If the ith and jth agents have access to the relative information $x_i - x_j$, then the nodes i and j in the graph are connected by a link. To simplify our analysis, we assign an orientation to the graph by denoting one of the nodes of each link to be the positive end. The choice of orientation does not change the results because the information flow is bidirectional. Suppose that ℓ is the total number of links and recall that the $n \times \ell$ *incidence matrix D* of a graph is defined as

$$d_{ij} := \begin{cases} +1 & \text{if node } i \text{ is the positive end of link } j \\ -1 & \text{if node } i \text{ is the negative end of link } j \\ 0 & \text{otherwise.} \end{cases} \quad (1)$$

The cooperative control problem studied in this paper is to achieve the following behaviors:

B1) Each agent reaches in the limit a common velocity vector $v(t) \in \mathbb{R}^p$ prescribed for the group:

$$\lim_{t\to\infty} |\dot{x}_i - v(t)| = 0, \quad i = 1, \cdots, n. \quad (2)$$

B2) The relative position of the two agents connected by link j:

$$z_j := \sum_{i=1}^{n} d_{ij} x_i \quad (3)$$

converges to a prescribed value z_j^d, $j = 1, \cdots, \ell$.

The set points z_j^d in B2 dictate the relative configuration of the group. When the graph contains cycles, the sum of the relative position vectors z_j over each cycle must be zero; that is, $z = [z_1^T, \cdots, z_\ell^T]^T$ must lie in the range space of $D^T \otimes I_p$ where $\otimes$ denotes the Kronecker product and I_p is the $p \times p$ identity matrix. We thus assume throughout the paper that $z^d = [(z_1^d)^T, \cdots, (z_\ell^d)^T]^T$ is designed to lie in the range space of $D^T \otimes I_p$, which means that

$$z^d = (D^T \otimes I_p) x_c \quad (4)$$

for some $x_c \in \mathbb{R}^{pn}$.

In this paper we assume that the agent dynamics are double integrators:

$$m_i \ddot{x}_i = f_i, \quad i = 1, \cdots, n \quad (5)$$

where m_i and f_i are the mass and the input force of agent i. For this dynamic model, the controller

$$f_i = -k_i(\dot{x}_i - v(t)) + m_i \dot{v}(t) - \sum_{j=1}^{\ell} d_{ij} \delta_j (z_j - z_j^d) \quad (6)$$

where k_i, $i = 1, \cdots, n$, and δ_j, $j = 1, \cdots, \ell$, are positive gains, achieves objectives B1-B2 above. This design is decentralized because $d_{ij} = 0$ for links j that are not associated with agent i. Although the model (5) and the controller (6) are linear, it is not difficult to extend the analysis of this paper to nonlinear systems using the *passivity* formalism introduced in [7].

Defining $x = [x_1^T, \cdots, x_N^T]^T$, $\Delta = \text{diag}\{\delta_1, \cdots, \delta_\ell\}$, $M = \text{diag}\{m_1, \cdots, m_n\}$, $K = \text{diag}\{k_1, \cdots, k_n\}$, and using the weighted Laplacian matrix $L_\Delta = D\Delta D^T$ of the graph (without the subscript "Δ", L denotes the *unweighted* Laplacian $L = DD^T$), we write the closed-loop dynamics (5)-(6) in the compact form:

$$(M \otimes I_p)\ddot{\mathbf{x}} + (K \otimes I_p)\dot{\mathbf{x}} + (L_\Delta \otimes I_p)\mathbf{x} = 0 \quad (7)$$

where

$$\mathbf{x}(t) := x(t) - x_c - \int_0^t 1_n \otimes v(\tau) d\tau, \quad (8)$$

x_c is as in (4), and 1_n denotes the n-vector of ones.

Note that objectives B1-B2 above translate to the asymptotic stability of the origin for

$$X = [\dot{\mathbf{x}}^T \quad \mathbf{z}^T]^T \quad (9)$$

where

$$\mathbf{z} = (D^T \otimes I_p)\mathbf{x} = z - z^d. \quad (10)$$

We write the dynamics (7) in the X-coordinates as

$$\dot{X} = \left[\begin{pmatrix} -M^{-1}K & -M^{-1}D\Delta \\ D^T & 0 \end{pmatrix} \otimes I_p \right] X \quad (11)$$

and note that X is restricted to the following subspace of $\mathbb{R}^{np+mp}$:

$$\mathscr{S}_x = \{(\dot{\mathbf{x}}, \mathbf{z}) | \dot{\mathbf{x}} \in \mathbb{R}^{np}, \mathbf{z} \in \mathscr{R}(D^T \otimes I_p)\}. \quad (12)$$

Asymptotic stability for $X = 0$ then follows from the Lyapunov function $V_1 = \dot{\mathbf{x}}^T (M \otimes I_p) \dot{\mathbf{x}} + \mathbf{z}^T (\Delta \otimes I_p) \mathbf{z}$ and the LaSalle invariance principle.

III. Instability due to Switching Topology

A. Example

For kinematic models described by single integrator dynamics, switching topology has been studied in [1], [3] and the references therein, and stability under arbitrary switching has been ascertained for classes of coordination algorithms. In contrast, for the second order model (7), a switching communication topology can trigger instability as we now illustrate with an example.

Consider four agents with a bidirectional communication topology that switches between a ring graph and a complete graph. Let $M = I$, $K = kI$ and $\Delta = \delta I$ for some constants $k > 0$ and $\delta > 0$. Then, the closed-loop dynamics (7) become

$$\ddot{\mathbf{x}} + k\dot{\mathbf{x}} + \delta(L_i \otimes I_p)\mathbf{x} = 0 \quad i = 1, 2 \quad (13)$$

where $L_i = D_i D_i^T$ is the Laplacian matrix for the ring graph when $i = 1$, and for the complete graph when $i = 2$.

Because L_1 and L_2 admit the same set of orthonormal eigenvectors q_j, $j = 1, \cdots, 4$ for their eigenvalues $\{0, 2, 2, 4\}$ and $\{0, 4, 4, 4\}$, respectively, the change of variables $d_j = (q_j^T \otimes I_p)\mathbf{x}$, $j = 1, \cdots, 4$ decouples the dynamics (13) into

$$\ddot{d}_j + k\dot{d}_j + \delta \lambda_{j_i} d_j = 0, \quad (14)$$

where λ_{j_i} is the jth eigenvalue of the Laplacian L_i, $i = 1, 2$. It then follows from standard results in switching systems [13], [14], [15] that, if the damping k is small, and if $\delta \lambda_{j_1} < 1$ and $\delta \lambda_{j_2} > 1$, then (14) is destabilized by a switching sequence that selects $i = 1$ when $d_j^T \dot{d}_j > 0$ and $i = 2$ otherwise. Instability with this sequence follows from the Lyapunov-like function $V = \|d_j\|^2 + \|\dot{d}_j\|^2$ which increases along the trajectories of (14). Because the eigenvalues λ_{2_i} and λ_{3_i} switch between the values 2 and 4 in our example, if $\delta \in (1/4, 1/2)$, then $\delta \lambda_{j_1} < 1$ and $\delta \lambda_{j_2} > 1$ indeed hold for $j = 2, 3$, thereby proving the existence of a destabilizing switching sequence.

We demonstrate this instability with a simulation in Fig. 1. We choose $p = 1$, take the reference velocity $v(t)$ in B1 in Section II to be zero and select the target vectors

z_j^d in B2 as zero to achieve the agreement of x_i's, $i = 1,\cdots,4$. Although the controller (6) guarantees agreement for any fixed connected graph, when the communication topology switches between a complete graph and a ring graph according to the sequence described above, Fig. 1 shows that the relative distances between the agents diverge.

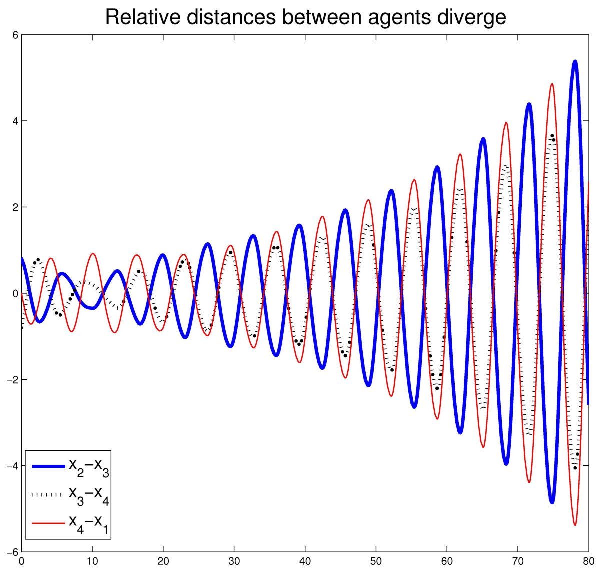

Fig. 1. A switching sequence described in Section III-A between the ring and complete graphs destabilizes the relative motion of the agents under the controller (6).

Since the dynamics (11) are exponentially stable, using the concept of dwell-time [13], [16], [17], we can ensure the stability of the origin of X if all graphs in the switching sequence are connected and if the interval between consecutive switchings is no shorter than some minimum dwell time $\tau > 0$, where estimates for τ can be obtained following [17]. In the next subsection, we employ the concept of an "average graph" to show that fast, periodic switching also preserves stability.

B. Fast Switching and Average Graph

Consider a periodic switching sequence $\sigma(t)$ in which the topology switches $N-1$ times, $N \geq 1$, during one period T. We label N graph Laplacians in T as L_Δ^i, $i = 1,\cdots,N$ and denote their dwell times by τ_i, $i = 1,\cdots,N$, $\sum_{i=1}^N \tau_i = T$. We thus study the switched system:

$$(M\otimes I_p)\ddot{\mathbf{x}} + (K\otimes I_p)\dot{\mathbf{x}} + (L_\Delta^{\sigma(t)}\otimes I_p)\mathbf{x} = 0 \qquad (15)$$

where

$$L_\Delta^{\sigma(t)} \in \{L_\Delta^1, L_\Delta^2, \cdots, L_\Delta^N\}. \qquad (16)$$

To determine the stability of (15)-(16), we investigate the eigenvalues of the state transition matrix evaluated over a period T:

$$\Xi(T,0) = e^{A_N\tau_N}\cdots e^{A_2\tau_2}e^{A_1\tau_1}, \qquad (17)$$

where

$$A_i = \begin{pmatrix} 0 & I_n \\ -M^{-1}L_\Delta^i & -M^{-1}K \end{pmatrix} \otimes I_p \qquad (18)$$

is the system matrix of (15) in the coordinates of $(\mathbf{x},\dot{\mathbf{x}})$, $i = 1,\cdots,N$. When τ_i's are small, we rewrite (17) as

$$\begin{aligned}\Xi(T,0) &= \prod_{i=1}^N [I + \tau_i A_i + O(\tau_i^2)] \\ &= I + \sum_{i=1}^N \tau_i A_i + O(T^2) \\ &= I + TA^{av} + O(T^2) \end{aligned} \qquad (19)$$

where

$$A^{av} = \begin{pmatrix} 0 & I \\ -M^{-1}L_\Delta^{av} & -M^{-1}K \end{pmatrix} \otimes I_p \qquad (20)$$

and

$$L_\Delta^{av} = \frac{1}{T}\sum_{i=1}^N \tau_i L_\Delta^i \qquad (21)$$

is the average of the N graph Laplacians during the period T.

Because the linear combination (21) preserves the structure of a Laplacian, L_Δ^{av} defines an average graph obtained by superimposing the individual graphs $i = 1,\cdots,N$. In this average graph, the links are weighted by τ_i/T, which represents the relative dwell time of each graph constituting the average. This means that, if the time-varying graph is *jointly connected* as in [1], then the averaged graph described by L_Δ^{av} is connected.

We finally show that, when T is sufficient small, connectedness of the average graph implies stability of (15)-(16). To see this, note from (19) that the eigenvalues of $\Xi(T,0)$ are given by

$$\kappa_i = 1 + T\lambda_i + O(T^2), \quad i = 1,\cdots,2n, \qquad (22)$$

where λ_i's are the eigenvalues of A^{av}. It follows from the analysis in Section II that if the graph induced by the averaged Laplacian L_Δ^{av} is connected, then all λ_i's have negative real parts, except the one, say λ_1, at zero. This zero eigenvalue results from the null space of A^{av}, spanned by $a = [1_n^T \quad 0_n^T]^T$, which is also the null space of A_i, $i = 1,\cdots,N$. We thus conclude that $\Xi(T,0)a = a$, which implies $\kappa_1 = 1$. Then, for sufficiently small T, κ_i in (22), $i = 2,\cdots,2n$, remain inside the unit circle and $\kappa_1 = 1$ corresponds to the motion of the center, thereby guaranteeing the asymptotic stability of the subspace spanned by $a = [1_n^T \quad 0_n^T]^T$. Note that convergence to this subspace guarantees objectives B1-B2 in Section II.

Lemma 1: Consider the closed loop dynamics (15)-(16) with a switching signal $\sigma(t)$ of period T. If the averaged graph induced by (21) is connected, then there exists a T^*, such that for $T < T^*$, the the subspace spanned by $a = [1_n^T \quad 0_n^T]^T$ is asymptotically stable. □

IV. Parametric Resonance

A. Example

To illustrate parametric resonance in its most basic form, in this example we study the cooperative system (7) with $M = I$, $K = kI$ and $\Delta = \delta I$. To further simplify the notation we consider the single degree-of-freedom case $p = 1$. The same analysis extends to $p > 1$ with the use of Kronecker algebra. The graph is now time-invariant but the link gain δ is perturbed by a cosine term $\varepsilon \cos \omega t$, thus leading to the closed-loop model

$$\ddot{\mathbf{x}} + k\dot{\mathbf{x}} + (\delta + \varepsilon \cos \omega t)L\mathbf{x} = 0. \tag{23}$$

Because the graph is undirected, the Laplacian matrix L is symmetric, its eigenvalues λ_i, $i = 1, \cdots, n$, are real and nonnegative, and L can be diagonalized by an orthonormal matrix Q:

$$Q^T LQ = L_d := \operatorname{diag}\{\lambda_n, \cdots, \lambda_1\} \tag{24}$$

where $\lambda_n \geq \lambda_{n-1} \geq \cdots \geq \lambda_1 = 0$. If the graph is connected, then only λ_1 is zero, and the corresponding column in Q is the vector $\frac{1}{\sqrt{n}} 1_n$. Thus, we let

$$Q = [S^T \ \frac{1}{\sqrt{n}} 1_n] \tag{25}$$

where S satisfies $SS^T = I_{n-1}$ and $S1_n = 0$, and decompose $\mathbf{x}$ as

$$\mathbf{x} = S^T d + \frac{1_n}{\sqrt{n}} c, \tag{26}$$

where $d \in \mathbb{R}^{n-1}$ and $c \in \mathbb{R}$.

The dynamics of c correspond to the evolution of the center of $\mathbf{x}$ and can be obtained by premultiplying (23) by $\frac{1}{\sqrt{n}} 1_n^T$:

$$\ddot{c} + k\dot{c} = 0. \tag{27}$$

The solution $c(t)$ approaches $\dot{c}(0)/k + c(0)$, which means that the time-varying link gains do not affect the motion of the center.

Next we derive the dynamic equations for d. Since $SS^T = I_{n-1}$, we obtain from (26) that

$$d = S\mathbf{x} \tag{28}$$

which, from (23), leads to

$$\ddot{d} + k\dot{d} + (\delta + \varepsilon \cos \omega t)SL\mathbf{x} = 0. \tag{29}$$

We further note from (26) that

$$SL\mathbf{x} = SLS^T d \tag{30}$$

and from (24)-(25) that

$$SLS^T = \bar{L}_d \tag{31}$$

where $\bar{L}_d = \operatorname{diag}\{\lambda_n, \cdots, \lambda_2\}$. Substituting (30)-(31) into (29), we obtain

$$\ddot{d}_j + k\dot{d}_j + (\delta + \varepsilon \cos \omega t)\lambda_{n+1-j} d_j = 0, \quad j = 1, \cdots, n-1, \tag{32}$$

which is a Mathieu equation [9], [10], [18] with the natural frequency $\sqrt{\delta \lambda_{n+1-j}}$. It then follows from standard results for the Mathieu equation that instability occurs when the frequency of the perturbation is around $\omega = 2\sqrt{\delta \lambda_i}/r$, $r = 1, 2, 3, \cdots$, for each $i = 2, \cdots, n$. When damping k is zero, parametric resonance occurs at these frequencies for arbitrarily small ε. For nonzero damping k, parametric resonance occurs for sufficiently large values of ε.

B. Coupled Mathieu Equations

In the previous example, the assumptions that $M = I$ and $K = kI$ played a crucial role in obtaining the decoupled Mathieu equations (32). We now remove this assumption and study the case where M, K and Δ in (7) are diagonal matrices with not necessarily identical entries. We then reveal parametric resonance with an analysis of *coupled* Mathieu equations as in [10, Section 5.4], [18], [11], [9]. When each link gain δ_i is perturbed by $\varepsilon \bar{\delta}_i \cos \omega t$, (7) becomes:

$$M\ddot{\mathbf{x}} + K\dot{\mathbf{x}} + D(\Delta + \varepsilon \cos \omega t \bar{\Delta})D^T \mathbf{x} = 0 \tag{33}$$

where $\bar{\Delta} = \operatorname{diag}\{\bar{\delta}_1, \cdots, \bar{\delta}_\ell\}$. Premultiplying by the inverse of M, we obtain

$$\ddot{\mathbf{x}} + M^{-1}K\dot{\mathbf{x}} + M^{-1}L_\Delta \mathbf{x} + \varepsilon \cos \omega t M^{-1} L_{\bar{\Delta}} \mathbf{x} = 0. \tag{34}$$

where $L_{\bar{\Delta}} = D\bar{\Delta}D^T$. The coordinate transformation $y = T^{-1}\mathbf{x}$, where T is composed of the eigenvectors of $M^{-1}L_\Delta$, then leads to

$$\ddot{y} + T^{-1}M^{-1}KT\dot{y} + \Lambda y + \varepsilon \cos \omega t T^{-1} M^{-1} L_{\bar{\Delta}} T y = 0, \tag{35}$$

in which

$$\Lambda = \operatorname{diag}\{\hat{\lambda}_n, \cdots, \hat{\lambda}_1\} \tag{36}$$

and $\hat{\lambda}_i$'s are the eigenvalues of $M^{-1}L_\Delta$. Because a similarity transformation brings $M^{-1}L_\Delta$ to the symmetric form $M^{-\frac{1}{2}} L_\Delta M^{-\frac{1}{2}}$, we conclude that $\hat{\lambda}_i$'s are real and nonnegative. Because the null space of D^T is spanned by 1_n, one of the eigenvalues of $M^{-1}D\Delta D^T$, say $\hat{\lambda}_1$, is zero and the corresponding column in T is 1_n. Similarly to (25)-(26), we rewrite T as

$$T = [S \quad 1_n] \tag{37}$$

and note that

$$\mathbf{x} = Ty = Sd + 1_n c \tag{38}$$

where $d \in \mathbb{R}^{n-1}$, and $c \in \mathbb{R}$ is the center of $\mathbf{x}$. Then, it follows from (35) and the decomposition (38) that

$$\ddot{y} + T^{-1}M^{-1}KT\dot{y} + \Lambda y + \varepsilon \cos \omega t T^{-1} M^{-1} L_{\bar{\Delta}} S d = 0, \tag{39}$$

since $1_n c$ lies in the kernel of D^T.

When the damping term K is small, the off-diagonal entries of $T^{-1}M^{-1}KT$ can be neglected, that is,

$$T^{-1}M^{-1}KT \approx \operatorname{diag}\{\bar{k}_1, \cdots, \bar{k}_n\} := \bar{K} \tag{40}$$

where $\bar{k}_i$ is the ith diagonal entry of $T^{-1}M^{-1}KT$. The dynamics in (39) can then be written as

$$\begin{pmatrix} \ddot{d} \\ \ddot{c} \end{pmatrix} = -\bar{K} \begin{pmatrix} \dot{d} \\ \dot{c} \end{pmatrix} - \Lambda \begin{pmatrix} d \\ c \end{pmatrix} - \varepsilon \cos \omega t \begin{pmatrix} S^* M^{-1} L_{\bar{\Delta}} S & 0 \\ \zeta M^{-1} L_{\bar{\Delta}} S & 0 \end{pmatrix} \begin{pmatrix} d \\ c \end{pmatrix} \tag{41}$$

where $T^{-1} = \begin{pmatrix} S^* \\ \zeta \end{pmatrix}$.

We note from (41) that the dynamics of d are decoupled from that of c and that stability of the relative motion of the agents is determined by the d-dynamics. Results for coupled

Mathieu equations in [9], [10], [18] applied to (41) indicate that parametric resonance occurs around the frequencies

$$\omega = \frac{2\sqrt{\hat{\lambda}_j}}{r}, \quad j = 2, \cdots, n, \quad r = 1, 2, 3 \cdots \tag{42}$$

and

$$\omega = \frac{\sqrt{\hat{\lambda}_j} \pm \sqrt{\hat{\lambda}_k}}{r} \quad j \neq k, \quad j, k = 2, \cdots, n. \tag{43}$$

For $\bar{K} \neq 0$, parametric resonance occurs at these frequencies if ε is sufficiently large. When (42) is satisfied, the corresponding mode, d_{n-j+1}, is excited and the resulting parametric resonance is called *Subharmonic Resonance*. The parametric resonance resulting from (43) is known as *Combination Resonance* because the excitation frequency ω is a linear combination of two natural frequencies $\sqrt{\hat{\lambda}_j}$ and $\sqrt{\hat{\lambda}_k}$ [18]. Such resonances are well studied in structural mechanics literature and are not further discussed here.

C. Fast Varying Perturbation

In the examples above instability occurs when the frequency of the perturbation interferes with the natural frequencies of the cooperative system. We now show that if the perturbation is fast enough (large ω), the origin of X is asymptotically stable. In the next subsection, we investigate slow perturbations.

Defining $\tau_f = \omega t$ and denoting

$$\frac{d(\cdot)}{d\tau_f} = (\cdot)', \tag{44}$$

we rewrite the perturbed model in (34) as

$$\omega^2 \mathbf{x}'' + \omega M^{-1} K \mathbf{x}' + M^{-1}(L_\Delta + \varepsilon \cos \tau_f L_{\bar{\Delta}})\mathbf{x} = 0. \tag{45}$$

Then, using the new variables $z_f = \mathbf{z}(\tau)/\omega$, and $v_f = \mathbf{x}'$, we obtain from (45) that

$$\begin{pmatrix} v_f' \\ z_f' \end{pmatrix} = \frac{1}{\omega} \underbrace{\begin{pmatrix} -M^{-1}K & -M^{-1}D(\Delta + \varepsilon \cos \tau_f \bar{\Delta}) \\ D^T & 0 \end{pmatrix}}_{A^f(\tau_f)} \begin{pmatrix} v_f \\ z_f \end{pmatrix}. \tag{46}$$

When ω is sufficiently large, the averaging method [12] is applicable to (46) and the average of $A^f(\tau_f)$ is given by

$$A^f_{av} = \frac{1}{2\pi} \int_0^{2\pi} A^f(t) dt \tag{47}$$

$$= \begin{pmatrix} -M^{-1}K & -M^{-1}D\Delta \\ D^T & 0 \end{pmatrix}, \tag{48}$$

which has been proved to be asymptotically stable in Section II. The following lemma is thus a consequence of [12, Theorem 10.4]:

Lemma 2: Consider the closed-loop system (33). There exists a $\omega_f > 0$ such that for $\omega > \omega_f$, the origin of X is asymptotically stable.□

D. Slowly Varying Perturbation

To analyze the system (34) with slowly varying perturbation (small ω), we look at its system matrix $A_s(t)$ in the X-coordinates:

$$A_s(t) = \begin{pmatrix} -M^{-1}K & -M^{-1}D(\Delta + \varepsilon \cos \omega t \bar{\Delta}) \\ D^T & 0 \end{pmatrix}. \tag{49}$$

For any fixed t, if $\Delta + \varepsilon \cos \omega t \bar{\Delta} > 0$, that is

$$0 \leq \varepsilon < \min_{i=1,\cdots,\ell} \frac{\delta_i}{\bar{\delta}_i}, \tag{50}$$

it follows from the results in Section II that the equilibrium $X = 0$ is asymptotically stable on $\mathscr{S}_x$, which implies that $A_s(t)$ restricted to $\mathscr{S}_x$ is Hurwitz.

We next evaluate the derivative of $A_s(t)$ as

$$\dot{A}_s(t) = \begin{pmatrix} 0 & \varepsilon\omega \sin \omega t M^{-1} D \bar{\Delta} \\ 0 & 0 \end{pmatrix} \tag{51}$$

and compute its 2-norm:

$$\|\dot{A}_s\| = \sqrt{\lambda_{max}(\dot{A}_s^T \dot{A}_s)} \tag{52}$$

$$= \varepsilon\omega |\sin(\omega t)| \sqrt{\lambda_{max} \begin{pmatrix} 0 & 0 \\ 0 & \Delta D^T M^{-2} D\Delta \end{pmatrix}} \tag{53}$$

$$= \varepsilon\omega |\sin(\omega t)| \lambda_{max}(\Delta D^T M^{-2} D\Delta) \tag{54}$$

$$\leq \varepsilon\omega \lambda_{max}(\Delta D^T M^{-2} D\Delta). \tag{55}$$

Since $\|\dot{A}\|$ is bounded, we conclude from [19, Theorem 3.4.11] that for sufficiently small ω or ε, the origin of X of the perturbed system (34) is asymptotically stable.

Lemma 3: Consider the closed-loop system (33). There exists a $\bar{u} > 0$ such that for $\varepsilon\omega < \bar{u}$, the origin of X is asymptotically stable. □

V. UNMODELED DYNAMICS

We consider the following closed loop system with unmodeled dynamics, $i = 1, \cdots, N$,

$$m_i \ddot{x}_i = C_i \xi_i \tag{56}$$

$$\varepsilon \dot{\xi}_i = A_i \xi_i + B_i f_i \tag{57}$$

where (57) represents the unmodeled dynamics, $\varepsilon > 0$, A_i is Hurwitz, and f_i is defined in (6). When ε is small, the unmodeled dynamics are fast. We further assume that the dc gain of the unmodeled dynamics is $C_i A_i^{-1} B_i = -I$ so that the reduced model obtained by setting $\varepsilon = 0$ in (56)-(57) is identical to (5). It then follows from standard singular perturbation arguments (see, e.g. [12, Example 11.14]) that there exists ε^* such that for $\varepsilon < \varepsilon^*$, the origin of X is asymptotically stable under the control (6).

To illustrate the dependence of ε^* on the graph and the mass inertia, we simplify the model in (56)-(57) by assuming $M^{-1}K = kI_p$, $\Delta = \delta I_\ell$, $A = -I_p$, $B = I_p$ and $C = I_p$:

$$m_i \ddot{x}_i = \xi_i \tag{58}$$

$$\varepsilon \dot{\xi}_i = -\xi_i + f_i. \tag{59}$$

Denoting $x=[x_1^T,\cdots,x_n^T]^T$, $\xi=[\xi_1^T,\cdots,\xi_n^T]^T$, $\bar{\xi}=(M^{-1}\otimes I_p)\xi$ and using (8), we rewrite (58)-(59) in the compact form:

$$\begin{pmatrix}\dot{\mathbf{x}}\\ \ddot{\mathbf{x}}\\ \dot{\bar{\xi}}\end{pmatrix}=\underbrace{\begin{pmatrix}0 & I_{n\cdot p} & 0\\ 0 & 0 & I_{n\cdot p}\\ -\frac{\delta}{\varepsilon}(M^{-1}L\otimes I_p) & -\frac{k}{\varepsilon}I_{n\cdot p} & -\frac{1}{\varepsilon}I_{n\cdot p}\end{pmatrix}}_{A}\begin{pmatrix}\mathbf{x}\\ \dot{\mathbf{x}}\\ \bar{\xi}\end{pmatrix}+\begin{pmatrix}0\\ -1_n\\ M^{-1}1_n\end{pmatrix}\otimes\dot{v}. \tag{60}$$

Then, using [4, Theorem 3], it is not difficult to show that the $3n$ eigenvalues of A are the roots of the following n characteristic polynomials:

$$s^3+\frac{1}{\varepsilon}s^2+\frac{k}{\varepsilon}s+\frac{\delta}{\varepsilon}\bar{\lambda}_i=0,\quad i=1,\cdots,n, \tag{61}$$

where $\bar{\lambda}_i$'s are the eigenvalues of $M^{-1}L$. A Routh-Hurwitz argument further shows that the exact stability region in the parameter space is given by

$$\varepsilon<\varepsilon^*=\frac{k}{\delta\bar{\lambda}_{max}}, \tag{62}$$

where $\bar{\lambda}_{max}$ is the maximal eigenvalue of $M^{-1}L$. For sufficiently small ε, (62) is satisfied and the design in (6) guarantees stability despite the unmodeled dynamics. Denoting $m_{min}=\min_i m_i$, we note that a conservative upper bound of $\bar{\lambda}_{max}$ is $\frac{n}{m_{min}}$, which implies from (62) that if $\varepsilon<\frac{km_{min}}{\delta n}$, the origin of X is stable.

Note that, since $\bar{\lambda}_{max}$ is the maximal eigenvalue of $M^{-1}L$, ε^* depends not only on the graph structure, but also on the mass distribution of the agents. To illustrate this dependence, we consider four agents with $k=2$, $\delta=1$ and $p=1$. We compare ε^*'s under two graphs as in Fig. 2. When $M=\text{diag}\{5,3,2,1\}$, we compute from (62) $\varepsilon^*=1.4797$ for the star graph and $\varepsilon^*=0.8154$ for the tree graph, which means that the star graph is more robust for this M. However, when $M=I_4$, $\varepsilon^*=0.5, 0.5858$, respectively, for the star graph and the tree graph, which implies that the star graph is now less robust.

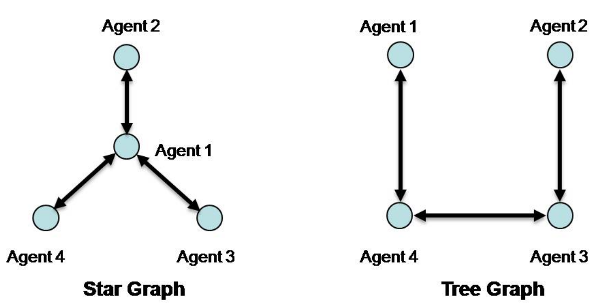

Fig. 2. The two graphs used in Section V to illustrate the dependence of ε^* on the graph structure and mass distribution.

CONCLUSIONS

For cooperative control technology to reach a mature state, its robustness properties and limitations must be fully understood. In this paper, we presented a preliminary investigation of robustness with respect to switching topology, link gain variation and unmodeled dynamics. We illustrated with an example that switching topology can lead to instability and showed that the closed-loop stability is maintained when switching is sufficiently fast or slow. We then revealed a parametric resonance mechanism by transforming the cooperative system with time-varying link gains into Mathieu equations. As in the case of switching graphs, stability is maintained when the perturbation is slow or fast enough that it does not interfere with the natural frequencies of the group dynamics. Our main goal in this paper was to attract attention to instability mechanisms rather than give complete recipes for robustness. Future work will pursue robust redesigns and extensions to nonlinear models and directed graphs.

REFERENCES

[1] A. Jadbabaie, J. Lin, and A. S. Morse, “Coordination of groups of mobile autonomous agents using nearest neighbor rules,” *IEEE Transactions on Automatic Control*, vol. 48, no. 6, pp. 988–1001, 2003.

[2] P. Ögren, E. Fiorelli, and N. E. Leonard, “Cooperative control of mobile sensor networks: Adaptive gradient climbing in a distributed network,” *IEEE Transactions on Automatic Control*, vol. 49, no. 8, pp. 1292–1302, 2004.

[3] R. Olfati-Saber and R. M. Murray, “Consensus problems in networks of agents with switching topology and time-delays.” *IEEE Transactions on Automatic Control*, vol. 49, no. 9, September 2004.

[4] J. A. Fax and R. M. Murray, “Information flow and cooperative control of vehicle formations,” *IEEE Transactions on Automatic Control*, vol. 49, no. 9, September 2004.

[5] H. Tanner, A. Jadbabaie, and G. Pappas, “Flocking in fixed and switching networks,” *IEEE Transactions on Automatic Control*, vol. 52, no. 5, pp. 863–868, 2007.

[6] R. S. Smith and F. Y. Hadaegh, “Closed-loop dynamics of cooperative vehicle formations with parallel estimators and communication,” *IEEE Transactions on Automatic Control*, vol. 52, no. 8, August 2007.

[7] M. Arcak, “Passivity as a design tool for group coordination.” *IEEE Transactions on Automatic Control*, vol. 52, no. 8, pp. 1380–1390, August 2007.

[8] D. Lee and M. W. Spong, “Stable flocking of multiple inertial agents on balanced graphs,” *IEEE Transactions on Automatic Control*, vol. 52, no. 8, pp. 1469–1475, August 2007.

[9] J. K. Hale, *Oscillations in Nonlinear Systems*. McGraw-Hill Book Company, Inc., 1963.

[10] A. H. Nayfeh and D. T. Mook, *Nonlinear Oscillations*. New York: John Wiley, 1979.

[11] J. K. Hale, *Ordinary Differential Equations*, 2nd ed. Robert E. Krieger Publishing Company, INC., 1980.

[12] H. Khalil, *Nonlinear Systems*, 3rd ed. Prentice Hall, 2001.

[13] D. Liberzon and A. Morse, “Basic problems in stability and design of switched system,” *IEEE Control Systems Magazine*, vol. 19, pp. 59–70, 1999.

[14] A. A. Agrachev and D. Liberzon, “Lie-algebraic stability criteria for switched systems,” *SIAM Journal on Control and Optimization*, vol. 40, no. 1, pp. 253–269, 2001.

[15] D. Liberzon, *Switching in Systems and Control*. Boston, MA: Birkhauser, June 2003.

[16] A. S. Morse, “Supervisory control of families of linear set-point controllers, part i: Exact matching,” *IEEE Transactions on Automatic Control*, vol. 41, no. 10, pp. 1413–1431, 1996.

[17] J. P. Hespanha and A. S. Morse, “Stability of swiched systems with average dwell-time,” in *Proceedings of 38th IEEE Conference on Decision and Control*, 1999.

[18] W.-C. Xie, *Dynamic Stability of Structures*. Cambridge University Press, 2006.

[19] P. A. Ioannou and J. Sun, *Robust Adaptive Control*. Prentice Hall, 1996.